

Optical Pulse distortion in Fibonacci-class Multilayer Stacks

A. ROSTAMI, S. MATLOUB

*Photonics and Nanocrystals Research Lab., Faculty of Electrical and Computer Engineering,
Tabriz University, Tabriz 51664, IRAN
e-mail: rostami@tabrizu.ac.ir*

Received 03.05.2005

Abstract

Optical pulse distortion and propagation through quasi-periodic structures generally and especially for Fibonacci-class, is investigated analytically and simulated numerically. In this analysis, the transfer matrix method (TMM) for distortion evaluation is used. The simulated results for Fibonacci-class quasi-periodic structures and pure periodic multilayer stacks are compared. We show that the Fibonacci-class quasi-periodic structure has a large dispersion coefficient with respect to a similar case in the periodic structure. So, quasi-periodic structures will destroy the incident pulse shape for smaller stack length than a periodic case in a similar situation. Finally, using output power, the distortion limit can be estimated and the maximum number of layers with acceptable distortion can be determined. Also, we have calculated the second order (D) and third order (B) dispersion coefficients for Fibonacci-class quasi-periodic structures around $1.55\mu m$ for dispersion compensation purposes.

Key Words: Pulse distortion, dispersion, quasi-periodic structures, and Fibonacci-class.

1. Introduction

Nowadays, high-speed and high capacity data communication is necessary for industrial requirements. Optical Fiber is one of the best alternatives as a physical device and backbone for high-speed communication. Therefore, interest in the analysis of linear pulse propagation through single mode optical fibers, waveguides, and fiber-based functional blocks has grown during recent years. Initially, this interest was driven by the aim of understanding and evaluating the effect that first-order chromatic dispersion had on the transmission and maximum attainable bit rate for the design of single mode fibers. Studies conducted at the end of the 1970s on the propagation of Gaussian pulses yielded useful expression for the link design. It was apparent that second order dispersion would be a limiting factor at those spectral regions where either first-order dispersion was small or vanished, in particular, at the second transmission window around $1.3\mu m$ for fiber that was the predominant region of operation of single mode fiber system in the early 1980s. Researchers then turned their attention to the evaluation of pulse propagation under this limiting factor. In a series of papers [1-3], Marcuse developed a closed formalism to evaluate the effect of first and second dispersion terms in the transmission of Gaussian pulses through single mode fibers, accounting for different types of single and multimode sources. Later, the advent of erbium-doped fiber amplifiers resulted in a new shift to the third transmission window, where first order chromatic dispersion was again the predominant

limiting factor; hence, many of the early results derived were directly applicable to both single-channel and wavelength division multiplexing systems. Recently, the demand for higher capacity, driven by current and future applications, has been pushing the research toward channel bit rates over 100Gbits/S and even in the terabits per second region, where transmission is possible only by low-order dispersion compensation. In this case, it is unclear what the limiting effects of higher-order dispersion terms will be. For this purpose [4,5], Amemiya has developed a general integral expression for the computation of the electric field impulse responses of an optical fiber due to higher-order, even, and odd dispersion orders. Also, there are many published papers considering the pulse propagation through optical fibers [6]. Considering the progress in optical applications, optical integrated circuits (OIC), and especially functional monolithic blocks, are so interesting for researchers working towards all-optical systems for increasing operation performance. For this purpose, determination of the optical pulse propagation through these structures is necessary; therefore, it is necessary to determine precisely the dispersion effect on pulse propagation through these systems. Optical periodic and quasi-periodic structures have important roles in the realization of functional blocks. In this paper, optical pulse propagation through Fibonacci-class quasi-periodic structures is investigated. Quasi-periodic structures have many important applications in applied and integrated optics [7-10]. Thus, the precise determination of distortion due to propagating through these functional blocks is critical and has an important affect on speed of data transmission. As such, we attempt to present semi-exact analysis for demonstrating the optical pulse propagation through Fibonacci-class quasi-periodic multilayer structures. In this analysis the transfer matrix method is used. Additionally, in this work, one-dimensional case will be considered.

The organization of this paper is as follows.

In section II, the mathematical treatment of pulse propagation through Fibonacci-class quasi-periodic structures is introduced. Results and discussion are presented in section III. Finally, the paper ends with a short conclusion.

2. Introduction to Fibonacci-class Quasi-periodic Structures-

In this section, we will first introduce the Fibonacci-class $FC(J, n)$ quasi-periodic structure. According to mathematical principles, in the Fibonacci sequence, there are two basic elements that are named A and B. The basic elements, A and B, are units in mathematical subjects, electrical, and optical engineering. Here, in our case, A and B are homogeneous slab waveguides with n_a , n_b , d_a , and d_b as the index of refraction for layer A, index of refraction for layer B, thickness for layer A, and thickness for layer B, respectively, which is demonstrated in Figure 1. There is a recursive relation for building Fibonacci-class structures, in terms of basic elements. Also, the recently generalized Fibonacci-class introduced is characterized by an index n . So, $FC(J, n)$ is a general demonstration of Fibonacci-class with class index J and generalized factor n .

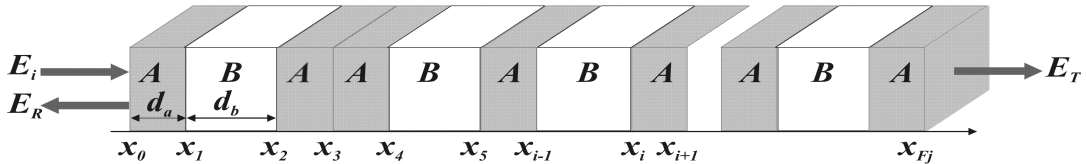


Figure 1. Schematics of Fibonacci-class Quasi-periodic Structures.

The $FC(J, n)$ sequence is a class of quasi-periodic lattice generated by substitution rules as

$$B \rightarrow B^{n-1}A, A \rightarrow B^{n-1}AB, \quad (1)$$

where n is a positive integer number and illustrates the generalized Fibonacci-class model factor. So, using Eq. (1), with starting from B, we have

$$\begin{aligned}
 S_1 &= B, \\
 S_2 &= B^{n-1}A, \\
 S_3 &= (B^{n-1}A)^n B,
 \end{aligned}
 \tag{2}$$

which follows the following recursion relation as

$$S_J = S_{J-1}^n S_{J-2}, \text{ for } J \geq 3. \tag{3}$$

As an example, if Eq. (3) is applied to $J = 3, 4, 5$, we obtain the following relations:

$$\begin{aligned}
 S_3 &= S_2^n S_1 \\
 &= (B^{n-1}A)^n B = (BB\dots BA)(BB\dots BA)\dots\dots(BB\dots BA)B \\
 S_4 &= S_3^n S_2 \\
 &= [(B^{n-1}A)^n B]^n (B^{n-1}A) \\
 S_5 &= S_4^2 S_3 \\
 &= [[(B^{n-1}A)^n B]^n (B^{n-1}A)]^n (B^{n-1}A)^n B.
 \end{aligned}
 \tag{4}$$

$$\tag{5}$$

Therefore, according to Eq. (2) and Eq. (3), generalized Fibonacci-class can be realized, and using traditional optical methods, such as TMM, one can obtain optical properties such as the reflection and transmission coefficients.

3. Principles of Pulse distortion estimation in Quasi-periodic Structures

In this section, we briefly describe the classic approach that is illustrated in Figure 2. The input time-domain field to the optical quasi-periodic waveguide, $E_{in} = E(z = 0, t)$, is given by the product of a slowly varying electric field envelop, $f(t)$, that corresponds to the modulating pulse defined by a time duration (T) and a high frequency chirped optical carrier, $\psi_0(t)$, as

$$E(0, t) = f(t)\psi_0(t),$$

$$\psi_0(t) = A(t)e^{j(\omega_0 t + \frac{ct^2}{2T^2})}. \tag{6}$$

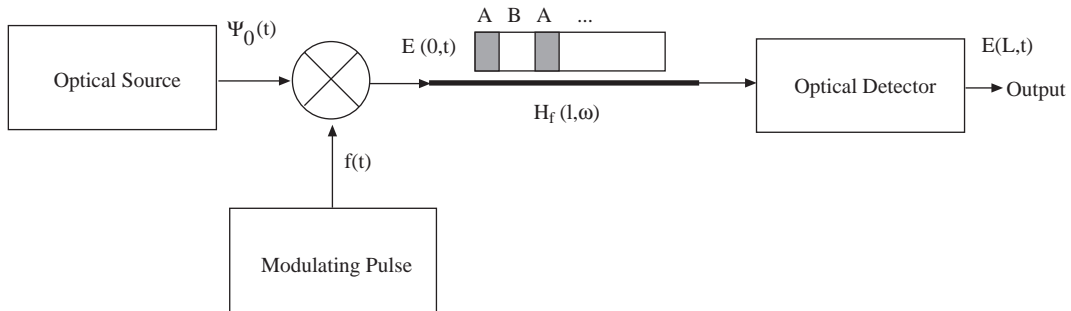


Figure 2. Schematics of Pulse propagation and distortion in Fibonacci-class Quasi-periodic Structures.

In Eq. (6), T represents the half-time duration of the input pulse that is related to its rms duration by $\delta_0 = \frac{T}{\sqrt{2}}$, $A(t)$ describes the un-modulated source random phase fluctuations that are related to its line width, ω_0 is the angular frequency corresponding to the optical carrier, and c is the so-called chirp parameter that characterizes the non constant instantaneous radian frequency of the light source, $\omega_i(t) = \omega_0 + \frac{c}{T^2}t$, that is present in most situations. The spectrum of the input field, $e(0, \omega)$, is given by

$$e(0, \omega) = \frac{1}{2\pi} \int_{-\infty}^{+\infty} f(t)\psi_0(t)e^{-i\omega t} dt = \int_{-\infty}^{+\infty} \Phi_0(s)F(\omega - s)ds \quad (7)$$

where $F(\omega)$ and $\Phi_0(\omega)$ are the Fourier transform of $f(t)$ and $\psi_0(t)$, respectively.

The optical quasi-periodic structure behaves as a linear medium as far as the propagation of the electrical field is concerned. Of course, the transverse magnetic field or longitudinal electric field can be considered similarly.

This means that the spectrum of the electric field after propagation through a length, L , $e(L, \omega)$, is obtained when we multiply Eq. (7) by the transfer function for the dispersive quasi-periodic structure that is given by $H_f(L, \omega)$, including system parameters and wave vector, $\beta(\omega)$. From this spectrum one can directly obtain the time-domain from the output electric field by means of an inverse Fourier transform:

$$E(L, \omega) = \int_{-\infty}^{+\infty} e(0, \omega)H_f(L, \omega)e^{i\omega t} d\omega. \quad (8)$$

Our final interest is in the evaluation of the ensemble average of the output intensity, because the detected photocurrent will be proportional to that magnitude. Note that the detection process produces a nonlinear relationship between the output electric field from the quasi-periodic structure and the output electric current. For estimation of the optical pulse distortion through a quasi-periodic structure, the following relation should be calculated:

$$\langle P(L, t) \rangle = \langle |E(L, t)|^2 \rangle \quad (9)$$

4. Mathematical Modeling of Optical Pulse Distortion in Quasi-periodic Structures- In this section, which is based on material presented in section 3, output power for estimation of distortion is calculated and the obtained relation is numerically simulated in section 5. Our method is based on transfer matrix method (TMM). According to this method, the reflection and transmission coefficients are calculated. In this work especially, we concentrate on Fibonacci-class quasi-periodic structures. Here, the proposed structure is linear and two transfer functions for describing this system are defined as:

$$H_{F.C.q.R} = \frac{E_R(0, \omega)}{E_i(0, \omega)},$$

$$H_{F.C.q.T} = \frac{E_T(L, \omega)}{E_i(0, \omega)}, \quad (10)$$

where E_i , E_R , E_T , $H_{F.C.q.R}$, and $H_{F.C.q.T}$ are the input, reflected, and transmitted signals, and the reflection and transmission transfer relations, which are functions of ω , L , d_a , d_b , n_a , n_b , α and $\beta(\omega)$, which are the incident light frequency, length of quasi-periodic structure, length of basic element A, length of basic element B, the index of refraction for first basic element, the index of refraction for the second basic element,

absorption coefficient, and system wave vector, respectively. In a simple case, for example, for optical fiber or homogeneous optical waveguides, the reflection transfer function is zero and the transmission transfer function can be expressed as $e^{-\alpha L + j\beta(\omega)L}$. Since the incident light pulse has gradual distribution in time and very narrow distribution in the frequency domain, we can expand the system wave vector in terms of Taylor series around central frequency and is given as:

$$\beta(\omega) = \beta_0 + \frac{1}{1!}\beta'(\omega - \omega_0) + \frac{1}{2!}\beta''(\omega - \omega_0)^2 + \frac{1}{3!}\beta'''(\omega - \omega_0)^3 + \dots \quad (11)$$

where, $\beta_0, \beta^{(n)}$ and ω_0 are the wave vector in central frequency, n^{th} derivative of the wave vector, and central frequency of the incident pulse, respectively. Moreover, the following parameters can be calculated based on the reflected transfer function and are defined as:

$$\tau = \frac{d\phi}{d\omega}, \quad (12)$$

$$v_g = \frac{1}{\beta'} = \frac{z}{\tau}, \quad (13)$$

$$\beta' = \frac{d\beta}{d\omega}, \quad (14)$$

$$\beta'' = \frac{d^2\beta}{d\omega^2} = -\frac{\lambda^2}{2\pi cz} \frac{d\tau}{d\lambda}, \quad (15)$$

$$\beta''' = \frac{d^3\beta}{d\omega^3} = \frac{\lambda^2}{(2\pi c)^2 z} \left[2\lambda \frac{d\tau}{d\lambda} + \lambda^2 \frac{d^2\tau}{d\lambda^2} \right], \quad (16)$$

$$D = \frac{\beta'' z}{2T^2}, \quad (17)$$

$$B = \frac{\beta''' z}{6T^3}, \quad (18)$$

where Eq. (12) demonstrates the delay time for pulse propagation from the reflection transfer function point of view. Eq. (13) presents the group velocity for traveling through a Fibonacci-class quasi-periodic structure after traveling in the z-direction at z. It can be obtained from delay time, which is defined in Eq. (12). Hence, the second expansion coefficient in Eq. (11) can be extracted using the reflection transfer function delay time. The third and fourth expansion coefficients are related to the reflection transfer function delay time using Eqs. (14 and 15). In addition, the standard definition for the second order dispersion (D) and third order dispersion (B) coefficients and their relations with the reflection transfer function delay time are presented in Eqs. (16 and 17). Consequently, based on these relations, we can conclude the dispersion properties of Fibonacci-class quasi-periodic structures based on numerical calculations of the reflection transfer function, its applications in dispersion compensation, and the limitation on the number of layers including system parameters.

Let us introduce the incident light pulse shape, introduced in section 4, and calculation algorithm. In this case, we apply the modulated Gaussian pulse as:

$$E_i = E_i(0, t) = f(t) \cdot \psi_0(t), \quad (19)$$

where

$$f(t) = e^{-\frac{t^2}{T^2}}, \quad (20)$$

and

$$\psi_0(t) = A(t)e^{i(\omega_0 t + \frac{\Delta\omega t}{2T}t)}, \quad (21)$$

where ω_0 , $A(t)$, T , and $\Delta\omega$ are the central frequency of the input pulse, amplitude of laser (including random phase fluctuations that related to the line-width, with very slow variation), the Gaussian pulse width, and the chirped factor for optical carrier, respectively. Now, we will introduce the pulse propagation through a Fibonacci-class quasi-periodic multilayer stack. For this purpose, we need to calculate the input pulse Fourier transform, which is expressed as:

$$\begin{aligned} E_i(0, \omega) &= \frac{1}{2\pi} \int_{-\infty}^{+\infty} f(t)\psi_0(t)e^{-i\omega t} dt \\ &= \int_{-\infty}^{+\infty} \Phi_0(s)F(\omega - s)ds \end{aligned}, \quad (22)$$

where $F(\omega)$ and $\Phi_0(\omega)$ are the Fourier transforms of $f(t)$ and $\psi_0(t)$, respectively. According to linear system behavior, the reflected light from a Fibonacci-class multi-layer stack can be obtained as:

$$E_R(0, t) = \int_{-\infty}^{+\infty} E_i(0, \omega)H_{F.C.q.R}(\omega, L, d_a, d_b, n_a, n_b, \alpha, \beta(\omega))e^{i\omega t} d\omega. \quad (23)$$

Eq. (23) should solve numerically and all required relations for the illustration of dispersion behavior must be calculated based on obtained relations in Eqs. (12) to (18). Moreover, the output average power is calculated according to the following relation and numerically from obtained data, respectively:

$$\langle P(0, t) \rangle = \langle |E_R(0, t)|^2 \rangle. \quad (24)$$

In the next section, we illustrate our simulation result for Fibonacci-class and periodic structures.

4. Results and Discussion

Here, we present the simulated results based on our proposed relations for demonstrating the pulse propagation and occurred distortion through a Fibonacci-class multilayer stack. Also, for comparison, we present simulated results for periodic cases. Our method is numeric and based on the transfer matrix method. Figures 3 and 4 are simulated results for Fibonacci cases, and the simulations for periodic cases are illustrated in Figures 5-7. In these figures, we report the reflection transfer function, the phase of this coefficient, delay time, second order dispersion coefficient (D), third order dispersion coefficient (B), and the reflected power.

As a first example, we consider the Fibonacci-class corresponding to $J=14$, including 378 layers and special parameters, which is given in the figure caption. For this case, Figure 3-a shows the reflection transfer function. Simulation parameters are tuned to obtain the reflected peak around 1.55 μm .

Using the numerical methods, the phase of the reflection transfer function is obtained and illustrated in Figure 3-b. It has a linear relationship versus incident wavelength, which is important and necessary for optical conditioners.

Time or group delay for this case is illustrated in Figure 3-c. The delay time for 1.55 μm is smaller than other wavelengths and is changed symmetrically.

The second order dispersion coefficient (D) is illustrated in Figure 3-d. When considering this figure, it is acknowledged that for these simulation parameters, the second order dispersion (D) at $\lambda_0 = 1.55\mu\text{m}$ is -0.79810 . Additionally, D is positive and changes to negative values in the simulation window.

In Figure 3-e, the third order dispersion coefficient is illustrated. As it is shown, around 1.55 μm there are two minimums. On the other hand, the sign of B is changed two times, which is important from compensation points of view.

Finally, the average reflected power for this case is illustrated in Figure 3-f. As it is shown, the reflected power is distorted totally and can't be related linearly to the incident light; so, the Fibonacci-class with these parameters and 378 layers can't be used as a signal conditioner.

As a second example, we try to reduce the number of layers in Fibonacci-class to 234 layers, which corresponds to $J=13$. We expect that in this case the distortion should be reduced. According to the previous example, the reflection transfer function is given in Figure 4-a. Furthermore, the system parameters are especially selected for peaking at 1.55 μm .

The phase of transfer function is given in part-b, and a linear relationship is observed for this case. If we compare the phase relation for two examples, Figure 3-b and Figure 4-b, we observe that in this case the linearity is better than the previous case. On the other hand, by lowering the number of layers, the transfer function has linear phase and the reflected light is more similar to incident light.

The time delay for $J=13$ is shown in Figure 4-c. As it is shown, the variation in this case is smaller than the $J=14$ case.

The second order dispersion coefficient (D) is shown in part-d (Figure 4-d). As it is shown around 1.55 μm , D changes linearly from negative values to positive values. The zero dispersion wavelengths can easily be controlled to lower or higher wavelengths. The slope of D depends on the number of layers. For the previous case, the slope of D is higher than this case. Also, the third order dispersion coefficient (B) is shown in Figure 4-e. In the previous case, we have two minimums for B between 1.5479-1.5529 μm , but in this case we have only one minimum. In this case, the minimum is between the two previous minimums, and the range of variation in this case is lowered in comparison to the previous case. Finally, the reflected power is displayed in part-f (Figure 4-f). As it is shown, the reflected power has distortion, in contrast to the previous case; nonetheless, there is distortion and it can't be ignored in some special cases. In any case, this case is better than the previous case.

As a final example for the Fibonacci-class, we consider a quasi-periodic case based on $J=12$. According to the previous cases, we illustrate the reflection transfer function (Figure 5-a), phase (Figure 5-b), delay time (Figure 5-c), the second (Figure 5-d) and third order (Figure 5-e) dispersion coefficients, and the reflected power (Figure 5-f). As it is shown, the reflected power is similar to the incident light and can be used as an optical conditioner.

For comparison of pulse distortion in Fibonacci-class quasi-periodic structures, here, the periodic structure is investigated for pulse distortion. As a first example, we consider the periodic case for $N=600$ layers. In part-a ((Figure 6-a)), the reflection transfer function is presented. In this case, the wavelengths lower than 1.55 μm are considered.

In part-b (Figure 6-b), the phase of the transfer function is illustrated and it has a linear relationship versus wavelength.

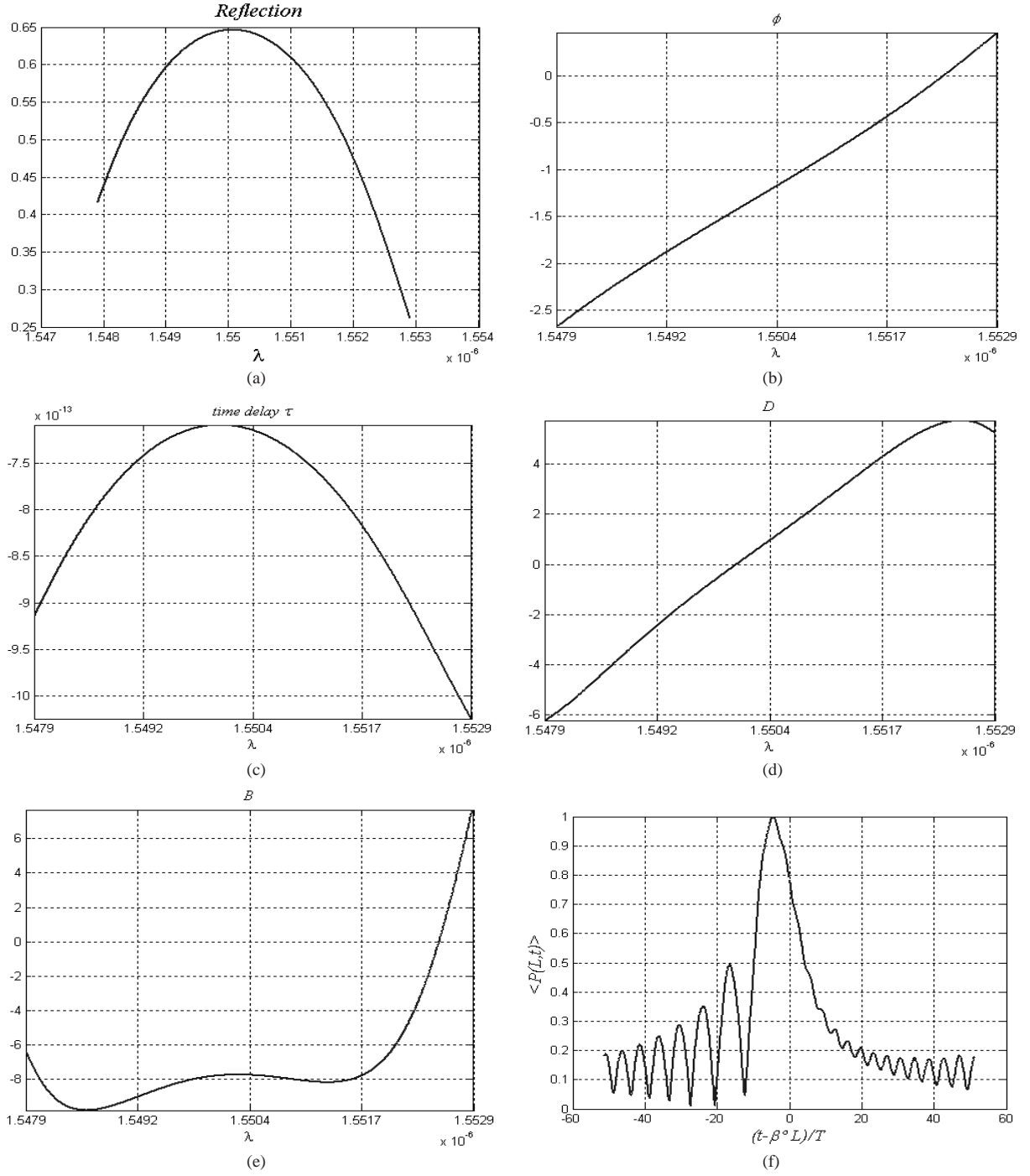


Figure 3. Simulation result for the Fibonacci-class a)- The Reflection Transfer Function, b)- The Phase function, c)-Time delay, d)-Second order Dispersion coefficient, e)- Third order Dispersion coefficient, and f)- Average Reflected Power.

$$\begin{aligned}
 J &= 14, N = 378 - \text{Layer}, \lambda_0 = 1.55\mu\text{m}, m = 0.2, L = 97\mu\text{m}, \\
 D &= -0.079810 \Big|_{\lambda_0} = 3.1, \sigma_0 = 0.1\text{Psec}, \\
 B &= -7.819408 \Big|_{\lambda_0} =, \frac{\sigma}{\sigma_0} = 28.672798, n_b = 2.9, \\
 \text{deltab} &= \frac{\lambda_0}{2n_0}, d_b = 0.9964\text{deltab}, d_a = 0.99\text{deltab}
 \end{aligned}$$

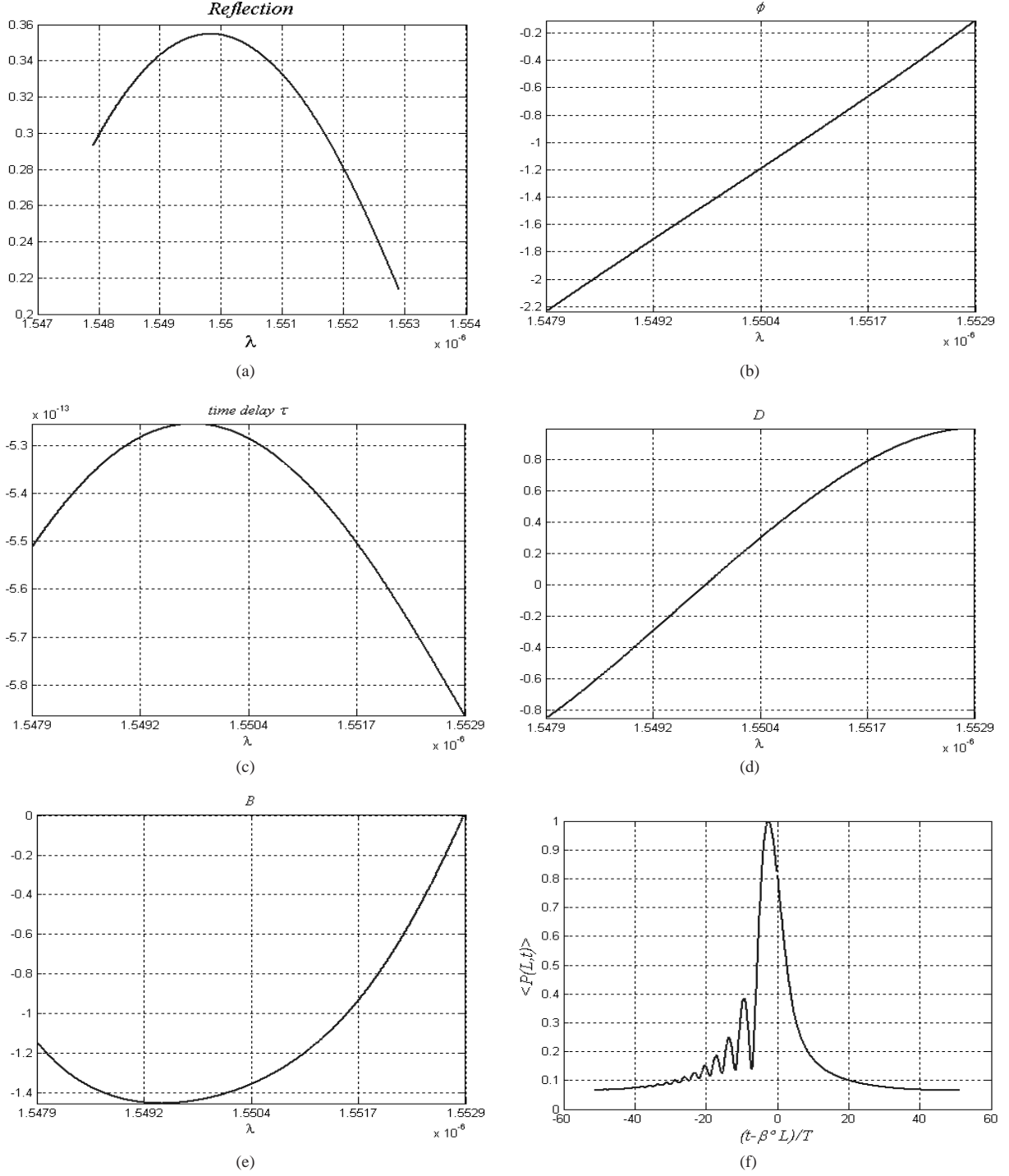


Figure 4. Simulation result for the Fibonacci-class a)- The Reflection Transfer Function, b)- The Phase function, c)-Time delay, d)-Second order Dispersion coefficient, e)- Third order Dispersion coefficient, and f)- Average Reflected Power.

$$\begin{aligned}
 J &= 13, N = 234 - \text{Layer}, \lambda_0 = 1.55\mu\text{m}, m = 0.2, L = 60\mu\text{m}, \\
 D &= 0.003969 \Big|_{\lambda_0}, n_a = 3.1, \sigma_0 = 0.1\text{Psec}, \\
 B &= -1.427894 \Big|_{\lambda_0}, \frac{\sigma}{\sigma_0} = 5.328157, n_b = 2.9, \\
 \text{deltab} &= \frac{\lambda_0}{2n_0}, d_b = 0.9964\text{deltab}, d_a = 0.99\text{deltab}
 \end{aligned}$$

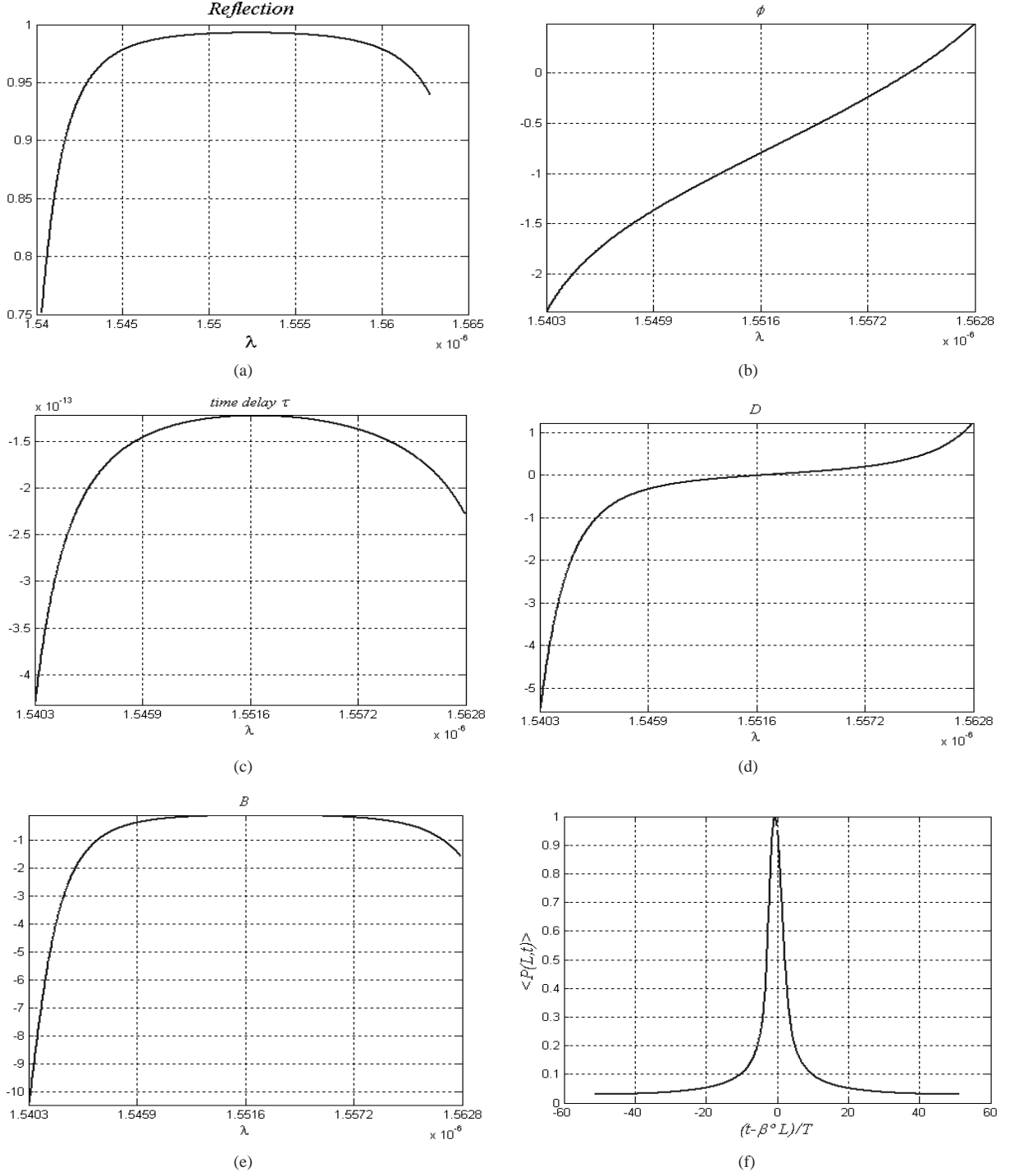


Figure 5. Simulation result for the Fibonacci-class a)- The Reflection Transfer Function, b)- The Phase function, c)-Time delay, d)-Second order Dispersion coefficient, e)- Third order Dispersion coefficient, and f)- Average Reflected Power.

$$\begin{aligned}
 J &= 12, N = 144 - \text{Layer}, \lambda_0 = 1.55 \mu\text{m}, m = 0.5, L = 37 \mu\text{m}, \\
 D &= -0.060613 \text{Bigl} |_{\lambda_0}, n_a = 3.25, \sigma_0 = 0.1 \text{P sec}, \\
 B &= -0.111386 \Big|_{\lambda_0}, \frac{\sigma}{\sigma_0} = 1.050658, n_b = 2.75, \\
 \text{deltab} &= \frac{\lambda_0}{2n_0}, d_b = 0.964 \text{deltab}, d_a = 0.99 \text{deltab}
 \end{aligned}$$

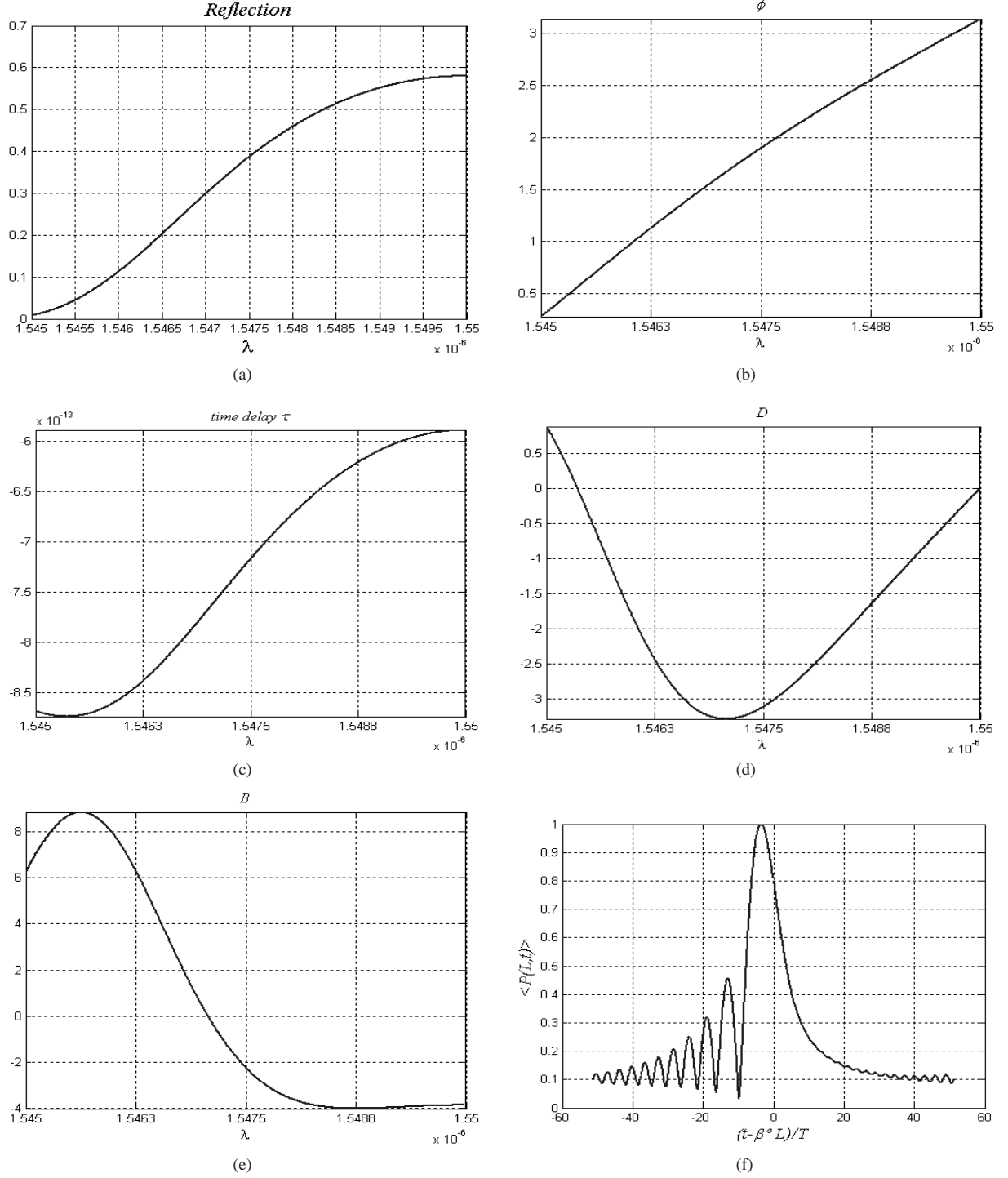


Figure 6. Simulation result for the Periodic Case a)- The Reflection Transfer Function, b)- The Phase function, c)- Time delay, d)-Second order Dispersion coefficient, e)- Third order Dispersion coefficient, and f)- Average Reflected Power.

$$\begin{aligned}
 N &= 600 - \text{Layer}, \lambda_0 = 1.55 \mu\text{m}, m = 0.01, L = 78 \mu\text{m}, \\
 D &= -0.006489 \Big|_{\lambda_0}, n_a = 3.01, \sigma_0 = 0.1 P \text{ sec}, \\
 B &= -3.887602 \Big|_{\lambda_0} \frac{\sigma}{\sigma_0} = 14.245531, n_b = 2.99, \\
 d_a &= d_b = \frac{\lambda_0}{2n_0}
 \end{aligned}$$

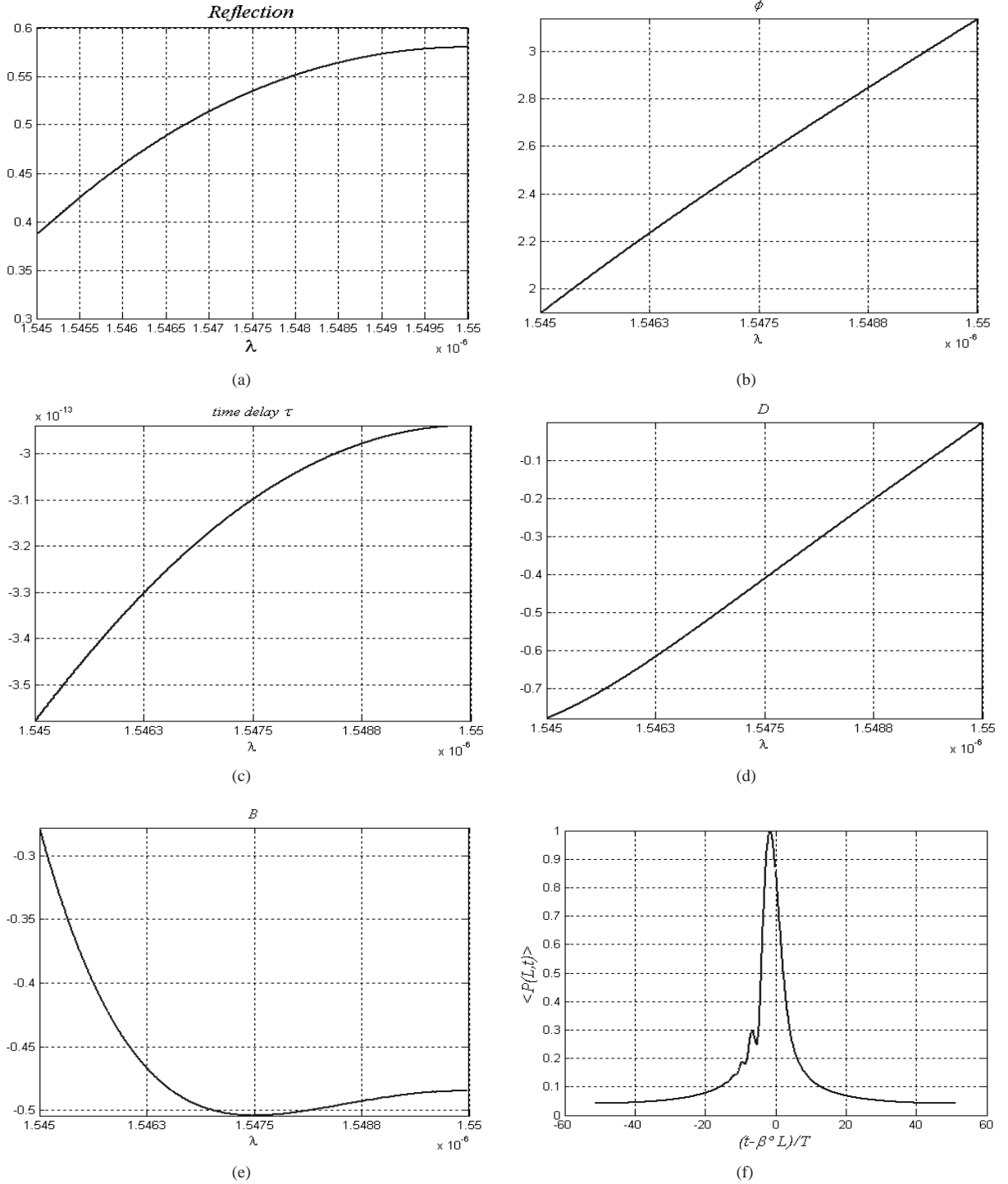


Figure 7. Simulation result for the Periodic Case. a)- The Reflection Transfer Function, b)- The Phase function, c)-Time delay, d)-Second order Dispersion coefficient, e)- Third order Dispersion coefficient, and f)- Average Reflected Power.

$$\begin{aligned}
 N &= 300 - \text{Layer}, \lambda_0 = 1.55 \mu\text{m}, m = 0.02, L = 39 \mu\text{m}, \\
 D &= -0.000842 \Big|_{\lambda_0}, n_a = 3.005, \sigma_0 = 0.1 P \text{ sec}, \\
 B &= -0.484795 \Big|_{\lambda_0} \frac{\sigma}{\sigma_0} = 2.038502, n_b = 2.995, \\
 d_a &= d_b = \frac{\lambda_0}{2n_0}
 \end{aligned}$$

The time delay for this case is presented in part-c (Figure 6-c).

The second order dispersion coefficient (D) for a periodic case is given in part d (Figure 6-d). For two wavelengths near 1.55 μm , D is zero and has a global minimum near 1.5470 μm . These values can be changed by changing the system parameters.

The third order dispersion coefficient (B) for this case is presented in part-e (Figure 6-e) and has constant values near 1.55 μm .

Finally, the reflected power is shown in part-f (Figure 6-f). As it is clear from this figure, the reflected power is distorted and can't be used as an optical conditioner.

As a second example, we consider the periodic case for $N=300$ (Figure 7). The simulation result is provided in Figure 7. We observe that the reflected power in this case is acceptable and has low distortion. According to our previous calculation, the reflection coefficient, phase, delay time, second and third order dispersion coefficients, and, finally, the reflected power are given in the following figures.

In this paper, we have shown that Fibonacci quasi-periodic structures have large dispersion coefficients and so, in the long run, compared to pure periodic mediums, will destroy input signal. Therefore, in the design of optical functional blocks, this subject should be considered.

5. Conclusion

In this paper, the analysis, including distortion properties of the optical pulse propagating through Fibonacci-class multilayer stack, has been presented. We have shown that in similar conditions, the dispersion coefficients of the Fibonacci-class have high value with respect to the periodic cases. So, the maximum number of layers in which the Fibonacci-class can be used for a given distortion level is smaller than the periodic case. Also, we have shown that with suitable control of parameters, the Fibonacci-class can be used as an optical dispersion compensator.

References

- [1] D. Marcuse, *Applied Optics*, **19**, (1980), 1653.
- [2] D. Marcuse, *Applied Optics*, **20**, (1981), 167.
- [3] D. Marcuse, *Applied Optics*, **20**, (1981), 3573.
- [4] M. Miyagi and S. Nishida, *Applied Optics*, **18**, (1979), 2237.
- [5] D. Marcuse, C. R. Menyuk and R. Holzlohner, *IEEE Photonic Technology Letter*, **11**, (1999), 75.
- [6] J. Capmany, D. pastor and S. Sales, *J. Opt. Soc. Am. B*, **20**, (2003), 2523.
- [7] A. Rostami and S. Matloub, *Laser Physics*, **14**, (2004), 1475.
- [8] A. Rostami and S. Matloub, *Proceeding of the AP-RSC2004, Qing Dao, China*, (2004).
- [9] X. Yang, Y. Liu and X. FU, *Phys. Rev. B*, **59**, (1999), 4545.
- [10] X. Yang and Y. Liu, *Eur. Phys. J. B*, **15**, (2000), 625.